VENTED HYDROGEN-AIR EXPLOSION IN A SMALL OBSTRUCTED RECTANGULAR CONTAINER: EFFECT OF THE BLOCKAGE RATIO

Xing Wang[1], Changjian Wang[1, 2] and Qiao Wang[1]

[1] **School of Civil Engineering, Hefei University of Technology, Hefei 230009, PR China, chjwang@hfut.edu.cn**

[2] **Anhui International Joint Research Center on Hydrogen Safety, Hefei 230009, China**

ABSTRACT

The explosion venting is an effective way to reduce hydrogen-air explosion hazards, but the explosion venting has been hardly touched in an obstructed container. Current experiments focused on the effects of different blockage ratios on the explosion venting in a small obstructed rectangular container. Experimental results show that three overpressure peaks are formed in the case with the obstacle while only two can be observed in the case of no obstacle. The obstacle blockage ratio has a significant influence on the peak overpressure induced by the obstacle-acoustic interactions, but it has an ignorable effect on the peak overpressure caused by the rupture of the vent film. The obstacle-induced overpressure peak first increases and then decreases with the increase of the blockage ratio. In addition, all overpressure peaks inside the container decreases with the increase of the vent area and its appearance time is relatively earlier for larger vent area.

Keywords: Hydrogen safety, Explosion, Blockage ratio, Overpressure

1. INTRODUCTION

Hydrogen as a promising energy carrier is considered to be one of the alternative fuels in future because of its ultra-low harmful emissions and high combustion efficiency. But the safety issue of the use of hydrogen has been paid more attention to, because of its extensive flammable range, low ignition energy and large burning rate etc. Any leakage of hydrogen in industries or laboratories, possibly results in an explosion, which can bring serious damage to people's life and property. Explosion venting is an effective method to release pressure of accidental explosions in confined spaces. So from the view of safety standpoint, vented explosion of hydrogen-air mixtures should be studied in more detail.

Usually, the obstacle results in flame acceleration and the increase of explosion overpressure in a closed container or tube [1-6]. For vented explosions, the obstacle also has a strong effect on the overpressure. The experiments performed by Bauwens et al. [7-9] in a vented container with the obstacle inside demonstrated the appearance of three pressure peaks. Wan et al. [10] studied the effect of blockage ratio ranging from 0% to 50% on the explosion of methane/air

mixtures, and found that the explosion intensity is very sensitive to the obstacle blockage ratio. Three blockage ratios (BR=36.4%, 49.8% and 71.7%) were investigated in Li et al.'s experiment [11], and it is found that the maximum flame speed, maximum overpressure, maximum rate of overpressure rise increase with the increase of the blockage ratio. Abdulmajid et al. [12] investigated the effect of the obstacle separation distance on the explosion. It was discovered that the obstacle with blockage ratio of 40% produces the highest explosion intensity However, the worst obstacle spacing was found to be shorter with increasing blockage ratio.

It is well known that the vent area is also important factor for vented explosion. Guo et al. [13] studied the effect of different vent area on internal venting overpressure and external flame, and found that the increase of vent area leads to the increase of the length of the maximum external flame and the decrease of peak pressure inside the vessel. Kumar [14] found that the internal peak pressure increases as hydrogen concentration increases for a given vent area. For a given hydrogen concentration, the internal peak pressure increases as the vent area decreases. However, an interesting issue was displayed in the experimental results of Ponizy and Leyer [15] that the venting overpressure shows a non-monotonic behavior with the increases of vent area.

Overall, Previous studies show the obstacle significantly affects the explosion overpressure of flammable gas in closed space. Few attention was paid to the combined effects of the obstructed geometry and the vent area on the explosion venting of hydrogen–air mixtures, which is more common in real scenarios. Moreover, such study is of practical significance for taking reasonable measures to deal with the complex hydrogen/air explosion accidents. To this end, the present tests were conducted in a rectangular channel with different blockage ratios and various vent areas. The results provide important data on the explosion venting associated with the effects of the blockage ratio and the vent area, especially compared to non-obstacle cases.

2. Experimental setup

Experiments were conducted in a steel rectangular container with the length of 500 mm and a cross section of 70 mm×70 mm, as shown in Fig.1. Two pieces of quartz glass were installed on both sides of the vessel to provide a 230 mm×70 mm optical path for view. The explosion flame evolution was visualized by high-speed schlieren system. The schlieren system consists of a light source, digital high-speed camera (NAC HX-3), two concave mirrors and a focusing lens. In experiment, the camera was operated at a 10000 frames per second and a 10μs shutter. Two piezoelectric pressure transducers were mounted on the vessel to record the pressure histories inside the vessel. PT1 was installed 20mm away from the ignition end while PT2 was placed 100 mm away from the vent. The pressure transducers were all coated with a thin layer of silicon grease to avoid thermal effect on the pressure measurements. Three repeated experiments for each case were performed in order to ensure the reliability of the measurements. The rear ignition was employed and the ignition energy was set to 9 J for each test.

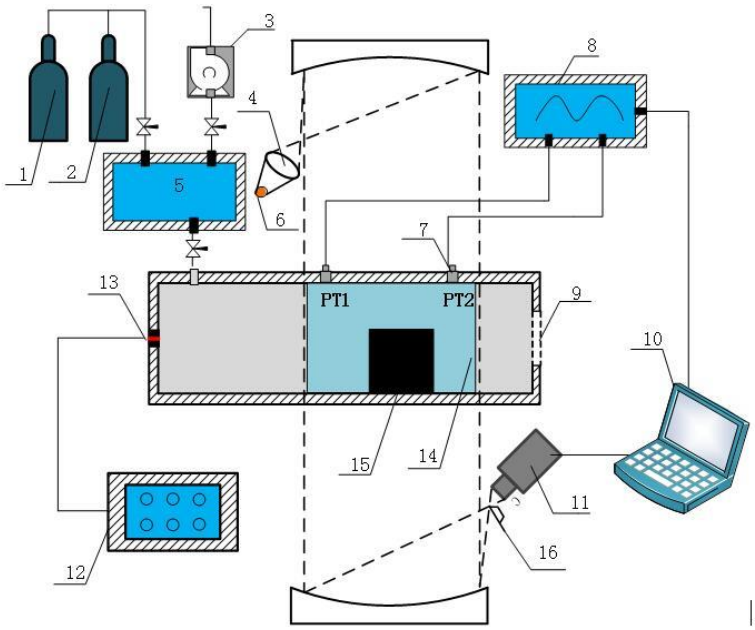

Fig.1. Experimental setup: (1) hydrogen cylinder, (2) air cylinder, (3) vacuum pump, (4) focusing lens, (5) gas distribution device, (6) light source, (7) piezoelectric pressure transducer, (8) data collector, (9) vent, (10) computer, (11) high-speed camera, (12) AC power, (13) Spark plug,（14）window, (15) Obstacle,（16）knife edge.

The vent was set on the one end of the vessel and covered by a thin polyethylene film with the low failure pressure. The obstacle had a size of 70mm (long) × 70 mm (width) with different height. It was placed at about 200mm away from the vent, and the distance was set about 93 mm between the right end of observation window and the obstacle. Five circular vent diameter (70mm, 50mm, 30mm, 10mm and 0mm) and six blockage ratios (28.6%, 42.8%, 57.1%, 64.2%, 71.4%, 85.7%) were tested in experiment. The vent burst overpressure of the 50 mm diameter vent was set as 29.7 kPa. The typical vent panel and the obstacle are shown in Fig 2. The premixed gas used in experiment consisted of 99.99% pure hydrogen and dry air, and the equivalence ratio was 0.5. The initial pressure and the temperature were 1 atmosphere and 298 K, respectively.

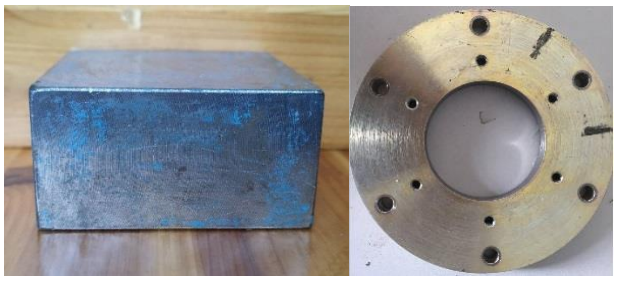

Fig.2. Obstacle (left) and the vent (right)

3. Experimental results and discussion

3.1. Effect of obstacle on the vented explosion overpressure

Fig. 3 shows the pressure profiles from the pressure sensor (PT2) in the cases with obstacle and obstacle-free. Two overpressure peaks can be observed in the absence of obstacle while there are three overpressure peaks in the case with the obstacle. For the case of no-obstacles, it is well known that the overpressure peak P0 is mainly related to several parameters, such as the vent burst pressure [16], the external explosion [18]. In the presence of the obstacle, the formation of pressure peaks is more complicated. According to previous studies [17], the formation reasons of the overpressure peak is mainly the relationship between the volume production rate by combustion and the discharged rate through the vent. In other words, the pressure rise is mainly the development of the volume production rate, while the discharged rate through the vent is favorable for the decrease of the pressure. Before the rupture of the film thickness, the pressure rises due to there is only a single volume production behavior caused by combustion inside the container. When the internal overpressure reaches 29.7 kPa (Vent burst overpressure), the vent film ruptures and the behavior of the discharged rate occurs. However, the pressure continues to increase until the pressure peak is reached 38kPa. Based on the previous study [16], in a short time of the polyethylene film rupture, the volume production rate produced by the combustion is still larger than the discharged rate through the vent. After the first overpressure peak P1, the pressure begins to decrease due to the effect of the discharged rate. It is strange that the pressure rebounds again over time, and resulting in the formation of the peak overpressure P3. Based on Bauwens et al.'s studies [18, 19], the formation of the peak overpressure P3 is mainly induced by the obstacle-effect. The reasons are as follows. The obstacle enhances the turbulence of the unburned gas and causes the increase of the flame surface, which leads to the instantaneous acceleration of the combustion rate of the unburned gas and further results in the larger volume production rate by combustion than the discharged rate through the vent. In addition, the phenomenon that the rise rate of P3 is significantly higher than that of P1 is observed in Fig.3 (B), which effectively confirmed that the acceleration of the volume production rate. Compared with P0, P1 and P3, P2 is much smaller in both cases and kept around several kilopascals, which is determined by the interactions between the acoustics and the container structure [18].

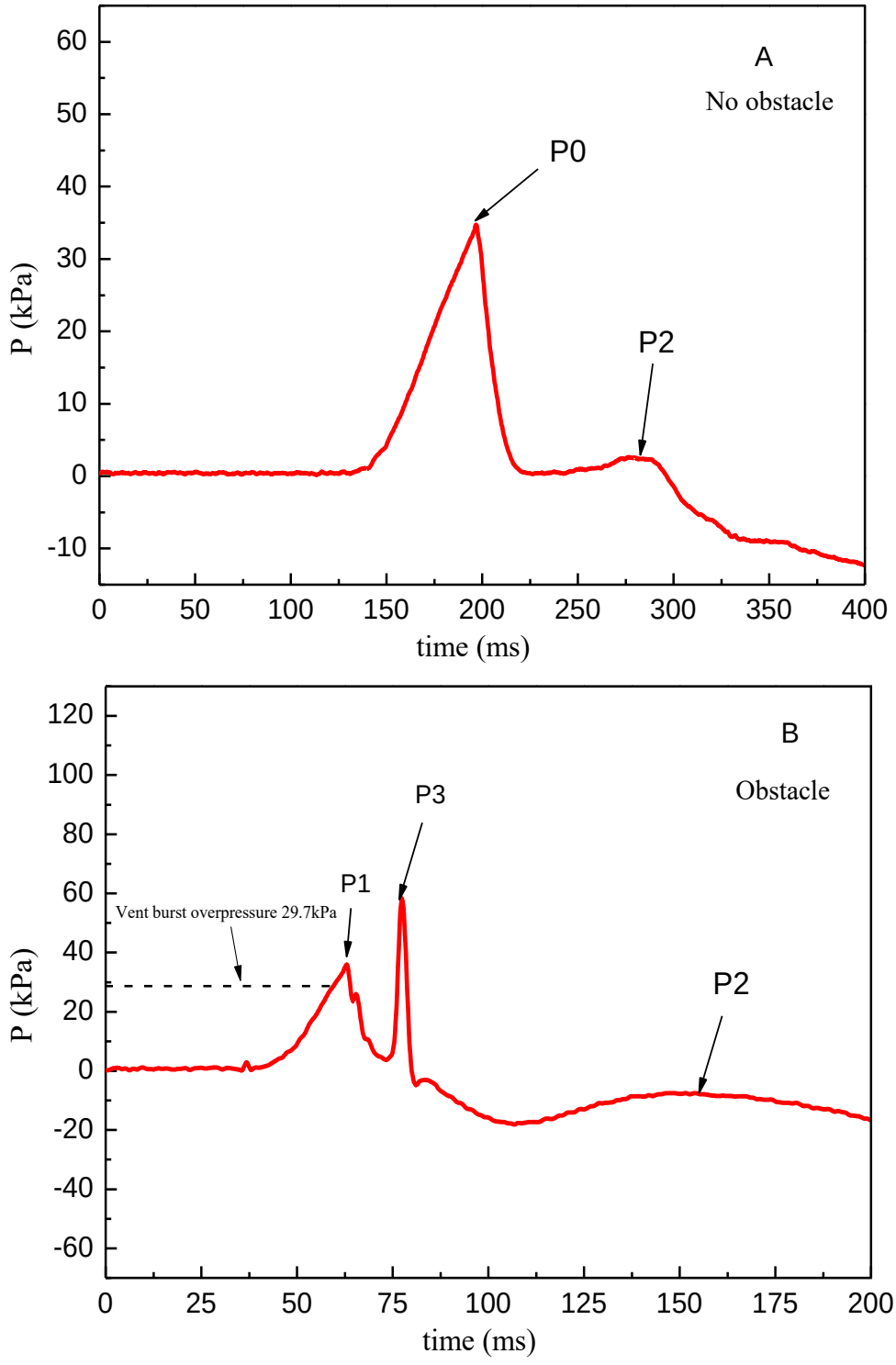

Fig.3. Typical overpressure histories at PT2 in the cases with no obstacle (A) and obstacle (B) (Blockage ratio: 35.7%; Vent diameter: 50mm).

3.2. Effect of the blockage ratio on the vented explosion overpressure

Fig. 4 shows the flame images for different blockage ratios. It is easily observed that the flame upstream of the obstacle is lifted by the obstacle. The time that the flame travels through the observation window in a vessel with an obstacle is shorter than that with no obstacle, which can be explained that the obstacle can enhance the flame propagation speed

for the former phenomenon [1, 5, 6]. Fig. 5 shows the flame tip position as a function of time at different blockage ratios. It should be noted that hydrogen equivalent ratio and vent diameter are 0.5 and 50mm, respectively. Since the flame propagates from right to left, the time that the flame arrives at the right end of the window was set as the start point. It is interesting found that, in the region marked with a blue line or in the upstream region, the blockage ratio smaller than 87.5% promotes the flame speed. The flame speed at a blockage ratio of 87.5% is significantly slower than those at other blockage ratios. But the flame speed always increases with the increase of the blockage ratio when it travels through the gap and in the downstream region. The possible reasons for explaining the effect of different blockage ratio on the flame propagation are as follows: (1) in upstream region, the reflection of acoustic waves induced by the combustion of the hydrogen/air mixtures on the obstacle dominates the flame acceleration. Different blockage ratio demonstrates different reflection ability to the acoustic waves. When the blockage ratio is less than a certain critical value, the obstacle facilitates the increase of flame speed, and otherwise it prohibits the latter. In a word, the flame propagation speed upstream of the obstacle is mainly determined by the blockage ratio. (2) The blockage ratio affects the strength of the shear layer attached the right corner of the obstacle, and further determines the strength of the induced instabilities. (3) After the flame passes through the gap between the top wall and the obstacle, the vortex induced by the left corner of the obstacle with different blockage ratio exerts different effect on the flame. As to both (2) and (3), in current case, larger blockage ratio can accelerate the flame speed.

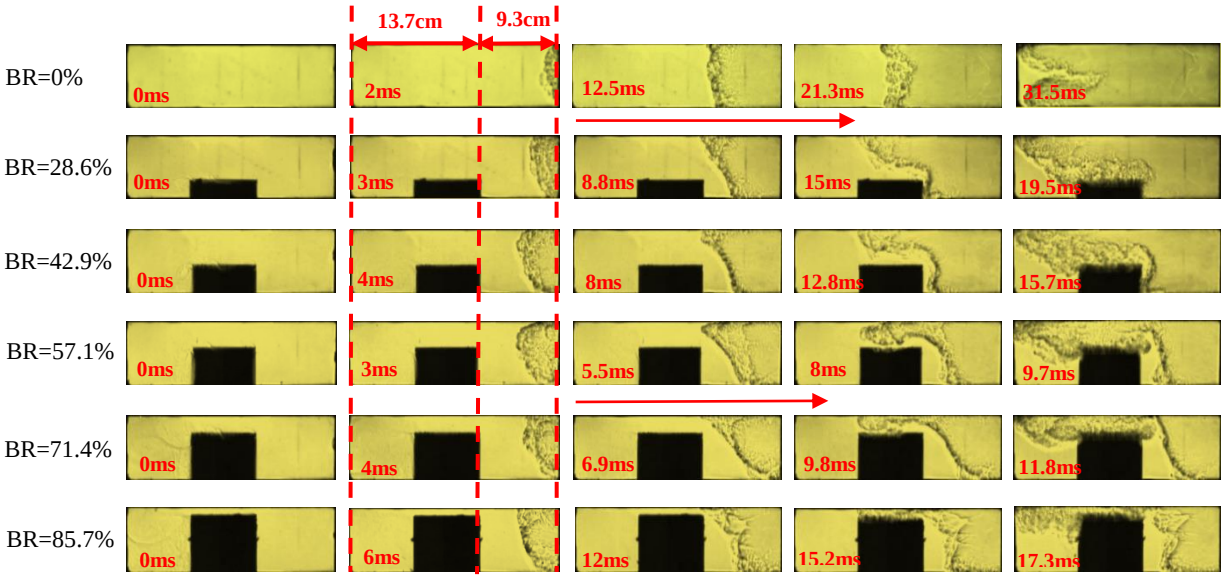

Fig.4. Flame images for different blockage ratio (vent area: 50mm).

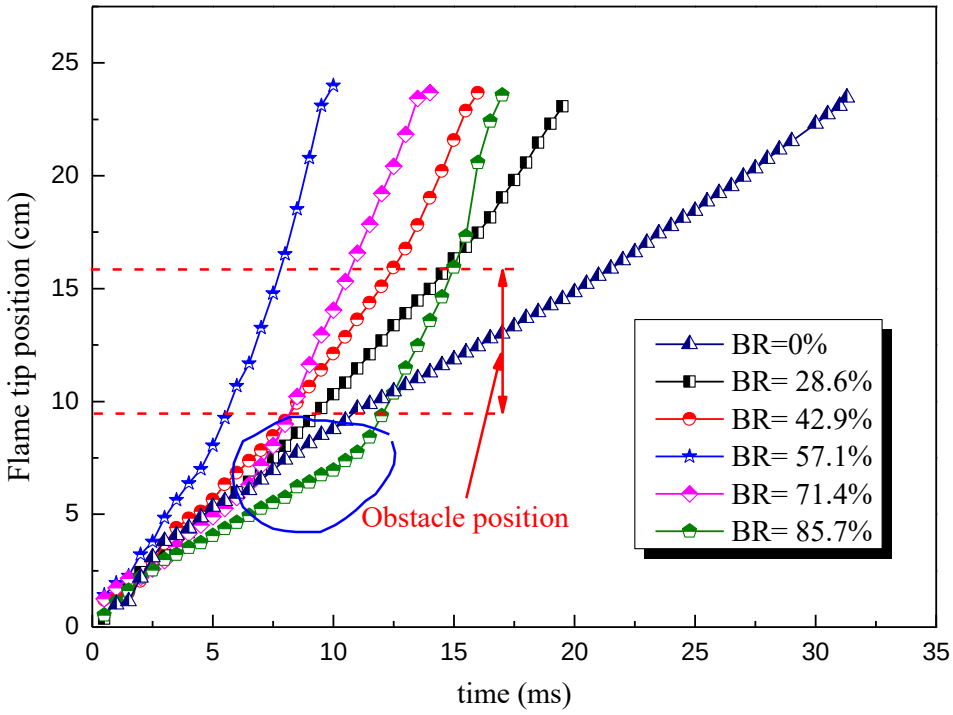

Fig.5. Flame tip position vs. time for different blockage ratio (vent diameter: 50mm).

In previous studies, the effect of the blockage ratio on the vented explosion overpressures P1 and P3 was hardly touched. Fig. 6 shows the pressure profiles from PT2 at different blockage ratios, while Fig.7 shows P1 and P3 as a function of the blockage ratio. It should be noted that hydrogen equivalence ratio ϕ=0.5 and vent diameter D=50mm are specified. It is easily observed that the occurrence time of the overpressure P3 first increases and then decreases with the increase of the blockage ratio. Simultaneously, the earlier P3 appears, the larger P3 is. According to previous studies [10, 11, 18], the turbulence of the unburned gas and the flame surface area are important parameter for the pressure formation in the combustion process, and the both depend mainly on the obstacle blockage ratio [10, 20]. At this point, the obstacle-effect enhances the turbulent intensity of the unburned gas and enlarges the contact area between the flame surface and the unburned gas, and further increases the combustion rate of the unburned mixture gas resulting in more energy to be released. In other words, different blockage ratios correspond to different values of P3. In current cases, the critical blockage ratio is 64.2%, where the overpressure P3 is the largest. However, P1 is not sensitive to the blockage ratio, implying that the blockage ratio has minimal influence on the venting overpressure P1. It is also interestingly found in Fig. 7 that the explosion overpressure P3 is less than P1 at the blockage ratio of BR=28.6% while P3 is larger than P1 at other blockage ratios. Therefore the effect of the blockage ratio on the vented explosion overpressure is not negligible, and moreover the maximum explosion overpressure is changeable with the blockage ratio.

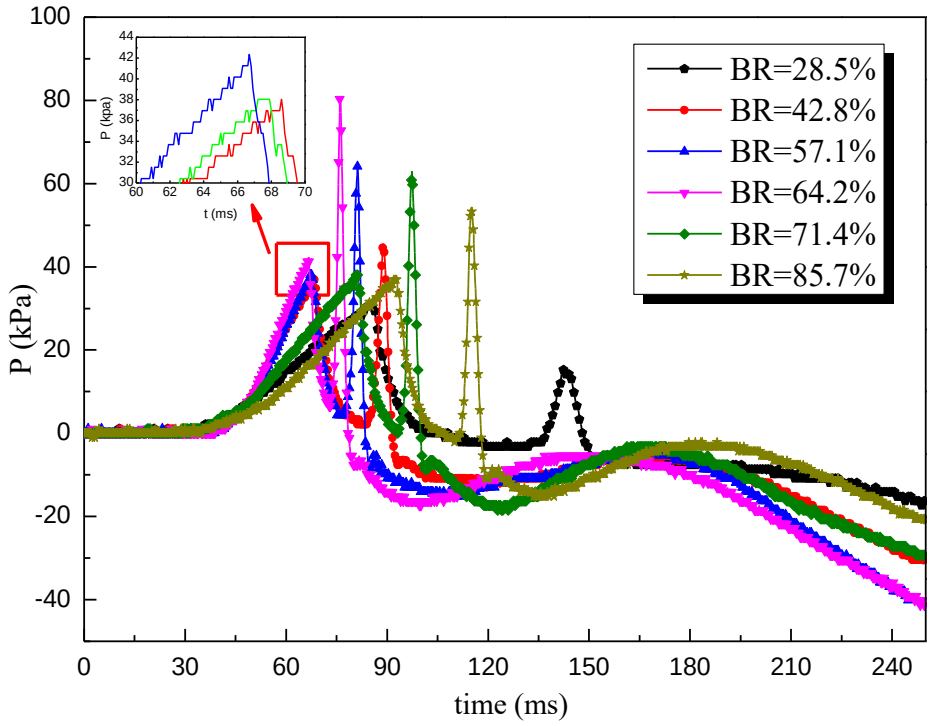

Fig.6. Overpressure vs. time for different blockage ratios (hydrogen equivalence ratio: 0.5; vent diameter: 50mm).

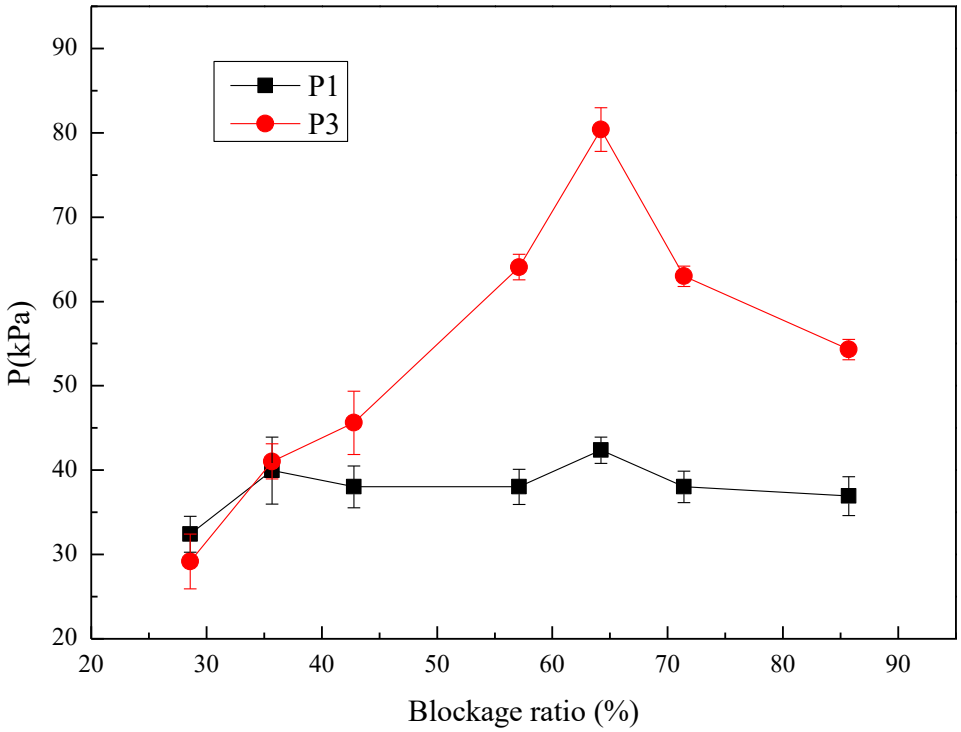

Fig.7. Overpressure peaks P1, P3 vs. blockage ratio (hydrogen equivalence ratio: 0.5; vent diameter: 50mm).

3.2. Effect of the vent area on the vented explosion overpressure

Fig. 8 plots that the overpressure profiles from PT1 with various vent areas while Fig. 9 presents the peak overpressure as a function of the vent area. It should be noted that no

obstacle is set in the container in these cases. It can be easily found that both the peak overpressure and its occurrence time decreases with the increase of the vent area. This are mainly attributed to the following two reasons. Firstly, the increase in the vent area leads to the decrease of the vent burst pressure for the same polyethylene film, which makes the maximum overpressure inside the container increase [16]. Secondly, it is well known that the burning rate remains constant for the hydrogen-air mixtures with the same concentration. In other words, the maximum overpressure inside the container increases with the decrease of the vent area, which is similar to those from Kumar [14] and Rocourt et al. [21], but different from that of Ponizy and Leyer [15]. Of course, the polyethylene film is broken earlier with the increase of the vent area, which results in more hydrogen-air mixture discharged outside of the container. With increasing the vent area, the time in which the discharge rate is larger than the volumetric rate produced by combustion occurs earlier and the internal overpressure decreases. Therefore, corresponding to the larger vent area, the pressure peak inside the container occurs relatively earlier.

In Fig. 9, the venting overpressure first drops rapidly and then slows down with the increase of the vent area. In other words, the significant increase in the vent area cannot always result in the significant decrease of the overpressure. A critical vent area which can cause the overpressure to be significantly decreased is a compromise in the engineering design. In current case, the vent diameter of 50mm is suggested since it leads to the decay of about 90% overpressure.

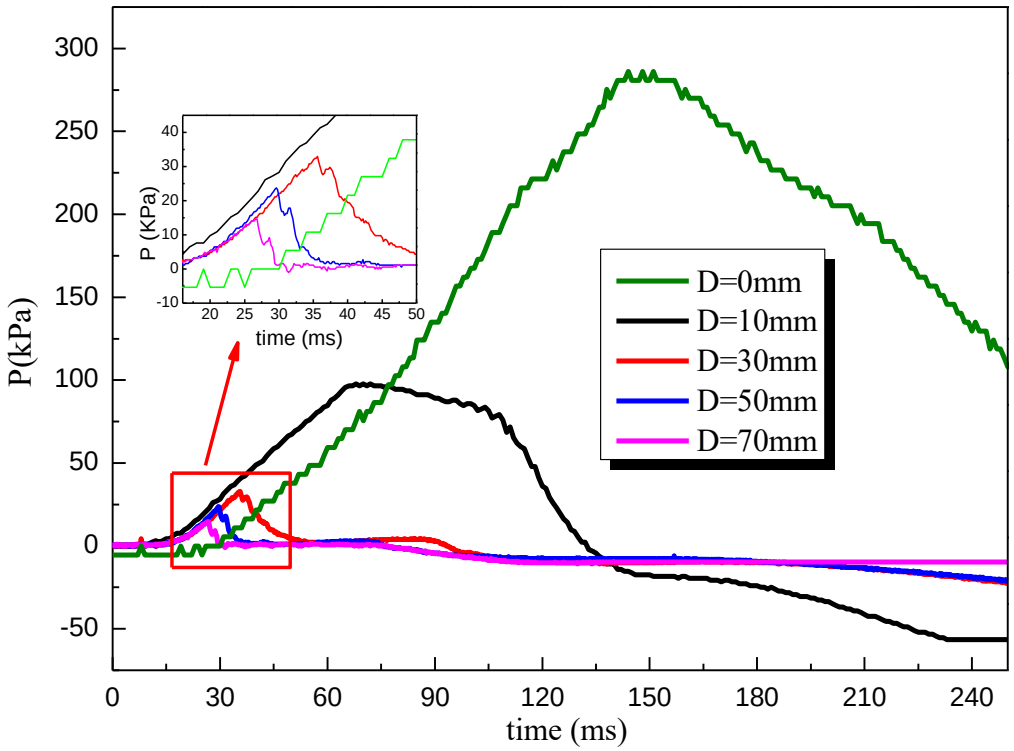

Fig.8. Overpressure vs. time for different vent diameters (hydrogen equivalence ratio: 0.5).

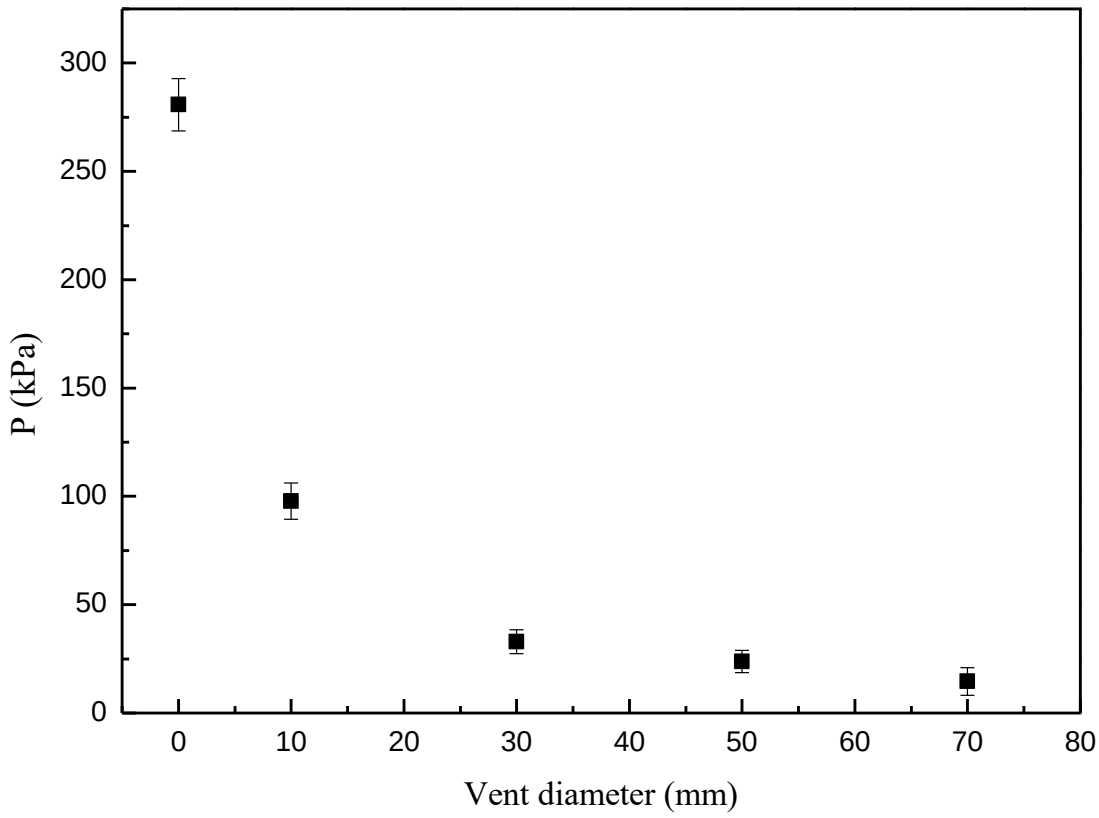

Fig.9. Overpressure vs. vent diameter in the cases with no obstacle (hydrogen equivalence ratio: 0.5).

In order to understand more the effect of the vent area on the vented explosion overpressure P1, P3 in the cases with the obstacle, the experiments with various the vent areas were performed and the typical results are shown in Fig.10. Similar to the cases with no obstacle, both P1 and P3 decrease with the increase of the vent area in the cases with the obstacle. It should be interestingly noted that the time difference between P1 and P3 increases with the vent area. Even only one peak overpressure was recorded by PT2 for the vent diameter of 10mm, which is similar to that in a closed vessel. This means that, once the vent area is decreased less than a critical value, the additional peak overpressure induced by the obstacle disappears or is merged to one. The reasons are as follows. The vent burst pressure increases with the decrease of the vent area, which provides a longer time for the unburned gas to be burn in the vessel and further release more energy to break the polyethylene film. Therefore, it can be observed clearly from the Fig.10 that the time of peak pressure formation was delayed, which is favorable to the resonance for the pressure peak P1 and the pressure peak P3 induced by the obstacle, resulting in a larger pressure peak. This implies that the additional peak overpressure (P3) is caused by the interactions between the size of the vent area and the obstacle.

In the region marked with a blue oval line in Fig. 10 (c), it can be found that the peak negative pressure from PT2 is larger than that from the PT1. Note that PT1 and PT2 are installed upstream and downstream of the obstacle, respectively, and PT2 is close to the vent. Due to the vent effect, the overexpansion of the burnt products is more significant in downstream region of the obstacle. Moreover, the obstacle can block the overexpansion of the burnt

products in upstream region of the obstacle. So these two main factors lead to larger peak negative pressure from PT2.

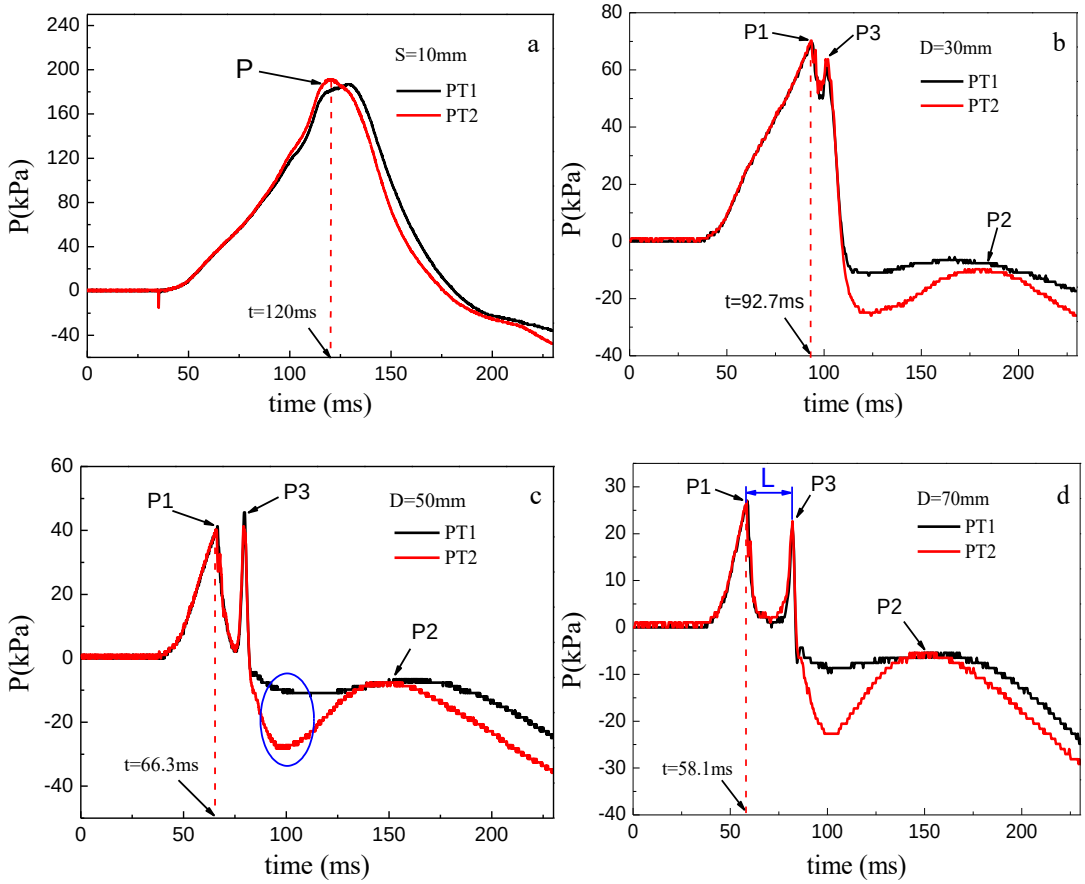

Fig.10. Overpressure vs. time in the case of different vent areas (blockage ratio BR=35.71%, hydrogen equivalence ratio:0.5).

Conclusions

In this paper, the experiments on the effects of vent area and obstacle ratio on vented explosion overpressure were conducted in a small rectangular container. The main conclusions can be drawn as follows. Compared with no-obstacle, the obstacle induces an additional peak overpressure P3. The blockage ratio significantly affects P3 while it has minimal effect on P1. P3 firstly increases and then decreases with the increase of the blockage ratio. Therefore the blockage ratio is an important parameter to determine the vented explosion overpressure. In the absence of an obstacle, the peak overpressure P1 decreases with the increase of the vent area, while the occurrence time of P1 is relatively earlier for larger vent area. In the case with the obstacle, both P1 and P3 decrease with the increase of vent area, and the occurrence time of P1 is also earlier for larger vent area. However, P1 and P3 merge into one as the vent area is reduced to a critical value, implying the obstacle cannot induce an additional peak overpressure as the vent area is small enough.

Acknowledgements

Financial support from the National K&D program special for inter-governmental cooperation (NO.2016YFE0113400) are sincerely acknowledged. The HySEA project receives funding from the Fuel Cells and Hydrogen 2 Joint Undertaking under grant agreement No. 671461. This Joint Undertaking receives support from the European Union's Horizon 2020 research and innovation programme and United Kingdom, Italy, Belgium and Norway.

References

[1] Abdulmajid M. NA'INNA* HNP, Gordon E. ANDREWS. Effects of obstacle separation distance on gas explosions: the influence of obstacle blockage ratio. Safety Science and Technology. 2014;84.

[2] I. O. Mone MD, R. Knystautas, and J. H. Lee. Flame Acceleration Due to Turbulence Produced by Obstacles. Combustion and Flame. 1980:39: 21-32.

[3] Johansen C, Ciccarelli G. Visualization of the unburned gas flow field ahead of an accelerating flame in an obstructed square channel. Combustion and Flame. 2009;156:405-16.

[4] Oran ES, Gamezo VN. Origins of the deflagration-to-detonation transition in gas-phase combustion. Combustion and Flame. 2007;148:4-47.

[5] Wang C, Huang F, Addai EK, Dong X. Effect of concentration and obstacles on flame velocity and overpressure of methane-air mixture. Journal of Loss Prevention in the Process Industries. 2016;43:302-10.

[6] Wingerden CJMV, Zeeuwen JP. Flame propagation in the presence of repeated obstacles_Influence of gas reactivity and degree of confinement Journal of hazardous materials. 1983;8:139-56.

[7] Bauwens CR, Chaffee J, Dorofeev SB. Vented explosion overpressures from combustion of hydrogen and hydrocarbon mixtures. International Journal of Hydrogen Energy. 2011;36:2329-36.

[8] Bauwens CR, Chao J, Dorofeev SB. Effect of hydrogen concentration on vented explosion overpressures from lean hydrogen–air deflagrations. International Journal of Hydrogen Energy. 2012;37:17599-605.

[9] Bauwens CRL, Bergthorson JM, Dorofeev SB. Experimental investigation of spherical-flame acceleration in lean hydrogen-air mixtures. International Journal of Hydrogen Energy. 2017;42:7691-7.

[10] Wan S, Yu M, Zheng K, Xu Y, Yuan Z, Wang C. Influence of obstacle blockage on methane/air explosion characteristics affected by side venting in a duct. Journal of Loss Prevention in the Process Industries. 2018;54:281-8.

[11] Li G, Du Y, Liang J, Wang S, Wang B, Qi S. Characteristics of gasoline–air mixture explosions with different obstacle configurations. Journal of the Energy Institute. 2018;91:194-202.

[12] Na'inna AM, Phylaktou HN, Andrews GE. Explosion flame acceleration over obstacles: Effects of separation distance for a range of scales. Process Safety and Environmental Protection. 2017;107:309-16.

[13] Guo J, Wang C, Liu X, Chen Y. Explosion venting of rich hydrogen-air mixtures in a small cylindrical vessel with two symmetrical vents. International Journal of Hydrogen Energy. 2017;42:7644-50.

[14] Kumar K. Vented Turbulent Combustion of Hydrogen-Air Mixtures in A Large Rectangular Vessel. Aiaa Journal. 2009 January 9-12.

[15] Ponizy B, Leyer JC. Flame dynamics in a vented vessel connected to a duct: 1. mechanism of vessel-duct interaction. Combustion Flame. 1999; 116: 259–71.

[16] Guo J, Wang C, Li Q, Chen D. Effect of the vent burst pressure on explosion venting of rich

methane-air mixtures in a cylindrical vessel. Journal of Loss Prevention in the Process Industries. 2016; 40:82-8.
[17] Cooper MG, Fairweather M, Tite JP. On the mechanisms of pressure generation in vented explosions. Combust Flame 1986; 65:1-14.
[18] Bauwens CR, Chaffee J, Dorofeev S. Effect of ignition location, vent size, and obstacles on vented explosion overpressures in propane-air mixtures. Combustion Science and Technology. 2010; 182: 1915-32.
[19] Chao, J., Bauwens, C.R., Dorofeev, S.B. An analysis of peak overpressures invented gaseous explosions. Proceedings of the Combustion Institute 2011; 33: 2367–2374.
[20] Li Q, Lu S, Xu M, Ding Y, Wang C. Comparison of Flame Propagation in a Tube with a Flexible/Rigid Obstacle. Energy & Fuels. 2016; 30:8720-6.
[21] Rocourt X, Awamat S, Sochet I, Jallais S. Vented hydrogen–air deflagration in a small enclosed volume. International Journal of Hydrogen Energy. 2014;39:20462-6.